A Numerical Case Study on the Sensitivity of Latent Heat-Flux and Cloudiness to the Distribution of Land-Use

Katja Friedrich and Nicole Mölders

Summary:

The accomplished case studies focus on the influence of land-use on the distributions of latent heat-fluxes and cloud-water. The numerical case studies were performed with the three-dimensional non-hydrostatic Mesoscale-Model GESIMA for different land-use distributions applying always the same initial conditions of a cloudy day in spring with a geostrophic wind of 8 m/s from the west. The cloud-water distributions at different times and at different levels, their temporal development, the daily sums of the domain-averaged latent heat-fluxes and cloud-water mixing ratios were investigated.

Even simple initial conditions (no orography, stable atmosphere) and simple pattern in the land-use distributions emphasize that the influence of surface heterogeneity on meteorological processes cannot be neglected. As shown in this case study, land-use distribution influences the distribution and the amount of cloud-water as well as the latent heat-flux. On the whole, all these processes are very complex and non-linear.

Zusammenfassung:

Die durchgeführten Sensitivitätsstudien konzentrieren sich auf den Einfluß der Landnutzungsverteilung auf die Flüsse latenter Wärme und das Wolkenwasser. Die numerischen Untersuchungen wurden mit dem dreidimensionalen nicht-hydrostatischen Mesoskalen-Modell GESIMA für verschiedene Landnutzungsmuster unter immer den gleichen meteorologischen Anfangsbedingungen für einen bewölkten Frühlingstag mit einem geostrophischen Wind von 8 m/s durchgeführt. Die Wolkenwasserverteilung zu bestimmten Zeiten und in bestimmten Niveaus, die zeitliche Entwicklung der Wolkenwasserverteilung, die Tagessummen der Gebietsmittelwerte der Flüsse latenter Wärme und des Wolkenwassers werden untersucht.

Auch einfache Randbedingungen (keine Orographie, stabile, atmosphärische Bedingungen) und einfache Landnutzungsverteilungsmuster machen deutlich, daß der Einfluß der Heterogenität der Unterlage auf meteorologische Prozesse nicht zu vernachlässigen ist. Sie kann entscheidend die Verteilungen der Flüsse latenter Wärme und des Wolkenwassers beeinflussen. Die damit verbundenen Prozesse sind äußerst komplex und nicht linear.

1. Introduction

The Progress and intensity of meteorological processes, e.g., evapotranspiration and the development of clouds, are controlled by many influences. These influences exist in different spatial and temporal scales that are often of subgrid-scale with respect to the grid-resolution of the models. This means they cannot be resolved by the model and, hence, have to be parameterised. The impact of surface characteristics and discontinuities on the atmospheric boundary layer (ABL) were investigated in many field experiments, theoretical and numerical studies (e.g., Anthes 1984, Avissar and Pielke 1989, Mahrt et al. 1994).

Several authors examined the influence of land-use distributions on the energy budget on the ground or on components of the energy budget. Mölders and Raabe (1996), for instance, showed that the grid resolution may strongly affect the calculated water and energy fluxes because a land-use type (being of subgrid-scale on a coarse grid and here of minor importance) may be dominant on a finer grid while using different horizontal grid resolutions and assuming the dominant land-use type within a grid box as the representative surface type

for the entire grid element. Jürrens (1996), for example, investigated the influence of wind on evapotranspiration. Herein, he used different grid resolutions and distributions of land-use which differ strongly or slightly in the roughness-length. The largest uncertainty in predicting evapotranspiration is provided in the case where the domains include land-use types with a high roughness-length (e.g., *forest*), and high wind-speed (10 m/s). Shuttleworth (1991) proposed two distinct scales of land-cover influence, namely, a 'disorganised' land surface, whose characteristic horizontal scales are less than 10 km, and an 'organised' land surface of characteristic length > 10 km. He theorised that only larger organised heterogeneity allows the atmosphere to develop a coherent response to land cover as substantiated by the formation of clouds and precipitation because the convective fluxes are aggregated over larger horizontal and vertical scales. These theoretical considerations were confirmed by the results of numerical simulations for which synthetic landscapes of various degrees of heterogeneity were assumed (Friedrich and Mölders 1998).

In our numerical case study, the influence of heterogeneity of land-use on the distributions of the latent heat fluxes as well as cloud-water is investigated under simple meteorological conditions. The differences of the latent heat-fluxes as well as cloud-water mixing ratios in the daily-sums of the domain-averages are also investigated. These investigations should serve as basic research on the impact of land-use heterogeneity to derive parameterisations of subgrid scale heterogeneity for use in numerical models of coarse grid-resolution.

2. Model Description and Initialisation

The Leipzig version of the non-hydrostatic meteorological model GESIMA (GEesthacht's SImulation Model of the Atmosphere; Kapitza and Eppel 1992, Eppel et al. 1995) is used to investigate the responses of water and energy fluxes as well as of cloudiness to the heterogeneity of the underlying surface. Its dynamical part is based on the anelastic equations. The physical features of the cloud module are based upon a five water-classes cloud-parameterisation scheme described in detail by Mölders et al. 1997. It considers the condensation of water-vapour, evaporation of cloud-water and rainwater, the formation of rainwater by melting of ice and graupel, autoconversion and coalescence. Moreover, the riming of supercooled cloud-water into ice crystals and graupel, the deposition of water-vapour onto ice and graupel, the conversion from ice crystals to graupel as well as sedimentation of rainwater, ice and graupel are taken into account. The treatment of the soil/vegetation/atmosphere interaction follows Deardorff (1978, see also Eppel et al. 1995), assuming homogeneous soil and land-surface characteristics within a grid cell. The surface stress and the near-surface fluxes of heat and water-vapour are expressed in terms of dimensionless drag and transfer coefficients applying the parametric model of Kramm et al. (1995). Above the atmospheric surface layer, the turbulent fluxes of momentum are calculated by a one-and-a-half-order closure scheme. Radiation transfer is calculated by a simplified two-stream method (Eppel et al. 1995).

A homogeneous flat terrain is assumed for all simulations. The model is initiated using profiles of air temperature and humidity typical for a cloudy day in spring. A geostrophic wind of 8 m/s from the west is assumed. The simulations are integrated for 24 hours where the first six hours serve as the adjusting phase. The whole test domain has a size of 75 x 75 km^2 with a horizontal resolution of 5 x 5 km^2. The vertical resolution varies from 20 m close to the ground to 1.5 km at the top. The model whole domain has a height of 10.5 km. Eight levels are located below the 2-km height and 7 are above.

All simulations are started with a geostrophic wind of 8 m/s from the west. Due to friction, the wind is reduced in speed to about 7 m/s and comes from west-southwest in the first level above ground. The terrain is assumed to be totally flat. Hence, in the case of heterogeneity, the differences in the near-surface wind field are mainly caused by the small differentials in the roughness length between a *grass*- or *sand*-land-use.

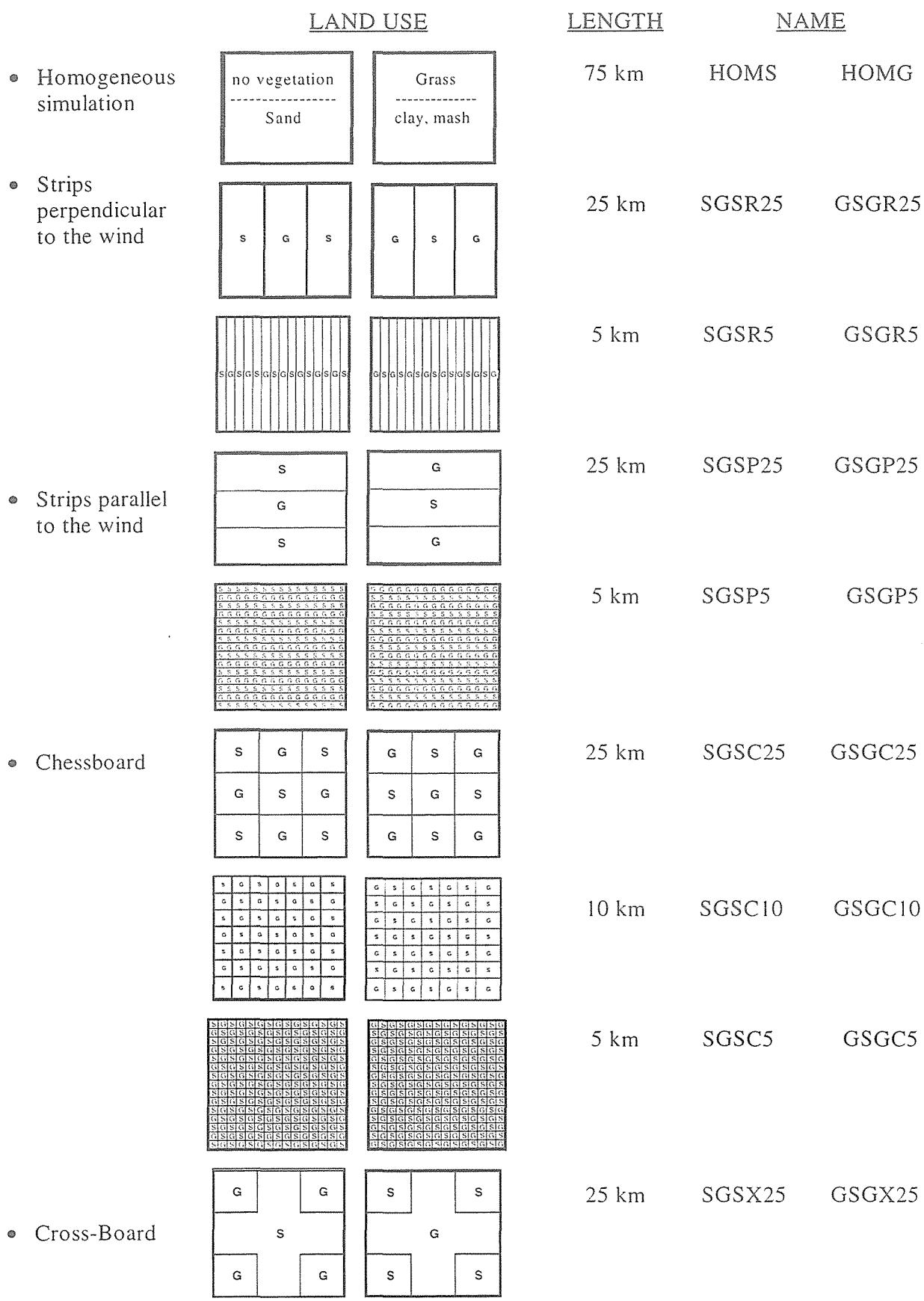

Fig. 1. Schematic view of the land-use distributions applied in the numerical experiments.

3. Design of the Numerical Experiments

The investigations are performed for different patches of a *sand /grass* mixture which differ not only in the amount but also in the heterogeneity. Sixteen simulations with heterogeneous land-surface conditions and two with homogeneous were performed. In the two simulations assuming homogeneous surface conditions, the entire domain is covered by *grass* or *sand*, respectively. These runs will be addressed as HOMG and HOMS hereafter. Eight simulations assuming heterogeneous land-surface conditions are performed with altering *sand* and *grass* strips equal in width to 25 km and 5 km, respectively. The strips are once orientated in a NS-direction perpendicular to the direction of the geostrophic wind and once in an EW-direction parallel to the geostrophic wind (Fig. 1). These runs are referred to as GSGP25, SGSP25, GSGR25, SGSR25, GSGR5, SGSR5, GSGP5, SGSP5, where G stands for *grass*, and S for *sand*, respectively. The letters P and R represent the orientation of the strips to the wind direction, namely, *parallel* and *perpendicular*. Furthermore, six simulations are carried out using a chessboard for which the squares have a length of 25 km, 10 km and 5 km (Fig. 1). These runs are referred to as GSGC25, SGSC25, GSGC10, SGSC10 (where the last east and the last south row have a 10 x 15 km² resolution), GSGC5, GSGC5, where G and S represent the *grass* and *sand* land-use as mentioned above, and C stands for *chessboard*, respectively. Two further simulations are performed with a north-south- and east-west-orientated cross which consists of five homogeneous 25 x 25 km^2 patches in the centre and four alternating 25 x 25 km^2 *sand* or *grass* patches on each corner (Fig. 1). These simulations are denoted as GSGX25 and SGSX25, respectively, where X stands for *cross*.

On summarising, the name of a simulation consists of six letters: the first three represent the land-use (GSG, SGS) while the last three letters stand for the patch size and the patch arrangement (Fig. 1). In the following discussion we use xxx representing all variations of land-use for a specific arrangement (xxxC25) or for all arrangements with a specific variation of land-use (SGSxxx).

4. The Daily-Sums of Domain-Averaged Latent Heat-Fluxes

In a recent paper, Friedrich and Mölders (1998) showed that for different degrees of surface heterogeneity the domain-averaged latent heat-fluxes may differ by several W/m² during the day. An enlargement of the latent heat-fluxes of 1 W/m² per day, however, will exceed the evapotranspiration of about 12.6 mm/a. At the *Lysimeterstation Brandis* near Leipzig (52.3°N; 12.6°E), for instance, the annual evapotranspiration amounts to 592 mm in an area with a lessivéy of loess soil and *grass*-clover-vegetation. Therefore, an error of about 10 W/(m²*d) in the daily estimate of evapotranspiration means an error of about 20.4 %/a in the annual evapotranspiration.

In this section, the influence of land-use distribution as well as patch-size on the daily- and domain-sums of latent heat-fluxes will be investigated. At noon the latent heat-fluxes calculated for the various artificial landscapes decrease with ever decreasing fractional coverage by *grass* (Tab. 1).

The largest differentials in the daily sums of the domain-averaged latent heat-fluxes (88 W/(m²*d)) occur between the results of the simulations with a homogeneous *grass*-cover (HOMG) and those with a homogeneous *sand*-cover (HOMS). The results of all simulations assuming heterogeneous surfaces arrange themselves between these two extreme values of latent heat-fluxes. Furthermore, the largest differentials between the simulations with a heterogeneous land-cover amount about about 50 W/(m²*d). In some simulations like GSGP5, GSGC25 and SGSP5 as well as GSGC5 and SGSC10, the daily sums of the domain-averaged latent heat-fluxes hardly differ. The daily sums of the domain-averaged latent heat-fluxes do not increase with increasing amounts of *grass* of the size of the *grass*-covered patches. Never-

theless, this does not mean that the latent heat-fluxes are not related to the patch-size or fractional coverage by *grass*.

Tab.1. Daily sums of domain-averaged latent heat-fluxes, domain-averaged latent heat-flux at 1200 LT, amount of *grass* and size of the largest *grass*-covered patch for all simulations.

Simulation	Daily sums of domain-averaged latent heat-fluxes (W/(m²*d))	Domain-averaged latent heat-flux at 1200 LT (W/m²)	Amount of *grass* (%)	Size of the largest *grass* covered patch (km²)
HOMG	404.6	44.9	100	5625
SGSX25	396.9	42.0	44.4	625
SGSC25	386.1	40.7	44.4	625
GSGP25	379.3	41.9	66.7	1875
SGSP25	378.5	40.0	33.3	1875
GSGR25	373.6	41.8	66.7	1875
SGSR5	370.1	41.1	46.7	375
GSGP5	368.9	40.9	53.3	375
GSGC25	368.6	40.7	55.6	625
SGSP5	368.4	40.9	46.7	375
GSGC5	366.1	40.5	50.2	25
SGSC10	366.0	40.5	48.0	150
GSGC10	361.8	40.5	52.0	150
GSGX25	358.9	39.7	55.6	3125
SGSC5	353.0	40.1	49.8	25
SGSR25	345.3	39.3	33.3	1875
GSGR5	343.9	39.5	53.3	375
HOMS	316.6	36.5	0	0

The largest deviations arise between HOMS and all other simulations, because a homogeneous dry and warm domain without vegetation partitions the incoming energy more towards higher sensible heat-fluxes than latent heat-fluxes. For small fractional coverage by vegetation, the latent heat-flux increases rapidly. The simulations with a patch orientation like a chessboard provide the smallest values of daily sums of the domain-averaged latent heat-fluxes at chessboard-sizes of 5 km followed by 10 km and 25 km. Surprisingly, in *sand*-majored simulations with large patch-sizes (e.g., SGSC25, SGSC10), the daily sums of domain-averaged latent heat-fluxes exceed those of their *grass*-majored counter-pairs (e.g., GSGC25, GSGC10).

Higher values of the daily sums of the domain-averaged latent heat-fluxes are often provided by the simulation without vegetation than by those with vegetation after sunset. At that time *sand* cools much faster than *grass*, dew might fall out, i.e., the water-vapour fluxes are directed downwards. In simulations with a smaller quadratic patch size (e.g., GSGC5, GSGC5), this process might be of no impact, because the squares are too small to yield an atmospheric response (Friedrich and Mölders 1998).

In simulations with strips orientated parallel to the wind (GSGP25, SGSP25, GSGP5, SGSP5), the daily sums of the domain-averaged latent heat-fluxes correlate with the size of the largest *grass* patch and the amount of *grass*. Here, the daily sums of the domain-averaged latent heat-fluxes increase with the patch-sizes and the fractional coverage by vegetation in the domain.

No correlation of the latent heat-fluxes to patch-size and arrangement are found in simulations with strips perpendicular to the wind. Comparing the results of these simulations with those from the simulations with the strips parallel to the wind shows that the different orientation to the wind causes differentials in the daily sums of the domain-averaged latent

Tab. 3 The amount of cloud-water in g/kg summarized between 250 m and 450 m. The grey squares are the daily sums of the domain-averaged cloud-water, while the values below this indicate the left column minus the top row and the values above the daily sums of the domain-averaged of values are the top row subtracted from the left column, respectively. Because of space limitations, all names have been shortened to the first two letters. Therefore, the first letter stands for the dominant land-use followed by the sign of the orientation of the patch and finally the length of the patch (see Fig. 1), respectively.

*g/(kg*d)*	*SX25*	*SC25*	*SC5*	*HOMG*	*GR5*	*GC10*	*GR25*	*SR5*	*GC5*	*SP5*	*SR25*	*GP5*	*GP25*	*HOMS*	*GC25*	*GX25*	*SC10*
SX25	**13.3**	-0	-0.6	-0.67	-0.7	-0.71	-0.7	-0.7	-0.7	-0.8	-0.8	-0.8	-0.8	-0.8	-0.8	-0.8	-1
SC25	-0	**13.3**	-0.6	-0.65	-0.7	-0.69	-0.7	-0.7	-0.7	-0.7	-0.7	-0.7	-0.7	-0.8	-0.8	-0.8	-1
SC5	-0.6	-0.6	**12.7**	-0.03	-0	-0.07	-0.1	-0.1	-0.1	-0.1	-0.1	-0.1	-0.1	-0.2	-0.2	-0.2	-0.4
HOMG	-0.7	-0.7	-0	**12.6**	-0	-0.04	-0	-0.1	-0.1	-0.1	-0.1	-0.1	-0.1	-0.1	-0.1	-0.1	-0.3
GR5	-0.7	-0.7	-0	-0	**12.6**	-0.04	-0	-0.1	-0.1	-0.1	-0.1	-0.1	-0.1	-0.1	-0.1	-0.1	-0.3
GC10	-0.7	-0.7	-0.1	-0.04	-0	**12.6**	-0	-0	-0	-0	-0	-0	-0.1	-0.1	-0.1	-0.1	-0.3
GR25	-0.7	-0.7	-0.1	-0.05	-0	-0.01	**12.6**	-0	-0	-0	-0	-0	-0	-0.1	-0.1	-0.1	-0.3
SR5	-0.7	-0.7	-0.1	-0.06	-0.1	-0.02	-0	**12.6**	-0	-0	-0	-0	-0	-0.1	-0.1	-0.1	-0.3
GC5	-0.7	-0.7	-0.1	-0.07	-0.1	-0.04	-0	-0	**12.6**	-0	-0	-0	-0	-0.1	-0.1	-0.1	-0.3
SP5	-0.8	-0.7	-0.1	-0.08	-0.1	-0.04	-0	-0	-0	**12.6**	-0	-0	-0	-0.1	-0.1	-0.1	-0.3
SR25	-0.8	-0.7	-0.1	-0.08	-0.1	-0.05	-0	-0	-0	-0	**12.6**	-0	-0	-0.1	-0.1	-0.1	-0.3
GP5	-0.8	-0.7	-0.1	-0.08	-0.1	-0.05	-0	-0	-0	-0	-0	**12.6**	-0	-0.1	-0.1	-0.1	-0.3
GP25	-0.8	-0.7	-0.1	-0.1	-0.1	-0.06	-0	-0	-0	-0	-0	-0	**12.5**	-0	-0	-0.1	-0.3
HOMS	-0.8	-0.8	-0.2	-0.14	-0.1	-0.1	-0.1	-0.1	-0.1	-0.1	-0.1	-0.1	-0	**12.5**	-0	-0	-0.2
GC25	-0.8	-0.8	-0.2	-0.14	-0.1	-0.1	-0.1	-0.1	-0.1	-0.1	-0.1	-0.1	-0	-0	**12.5**	-0	-0.2
GX25	-0.8	-0.8	-0.2	-0.15	-0.1	-0.11	-0.1	-0.1	-0.1	-0.1	-0.1	-0.1	-0.1	-0	-0	**12.5**	-0.2
SC10	-1	-1	-0.4	-0.35	-0.3	-0.31	-0.3	-0.3	-0.3	-0.3	-0.3	-0.3	-0.3	-0.2	-0.2	-0.2	**12.3**

heat-fluxes. Note that there exists an influence of wind-direction and wind-speed on the latent heat-fluxes (Jürrens 1996) as well as on cloud and precipitation formation (Mölders 1998).

Of all the heterogeneous simulations, simulation SGSX25 provides the largest daily sums of the domain-averaged latent heat-fluxes although it has not got the largest amount of vegetation (Tab. 1). The slightly warmer air, due to the stronger heating of the *sand* than of the *grass,* enhances evapotranspiration. On the contrary, the 'inverse landscape' GSGX25, which has a larger fractional coverage by *grass*, provides a small daily sum of the domain-averaged latent heat-fluxes because of the slightly cooler air in the lower ABL.

5. The Impact of Land-Use Distribution on Cloudiness

Different surface heterogeneity may yield to differences in water balances, a modified water supply to the atmosphere, and an altered temporal and spatial development of clouds. In this section, focus is on the development of clouds. In the synoptic situation simulated here, cloud bases are at a height of 250m and cloud tops are located at a height of 450 m above sea level (Note: the model basis is at sea level). In all simulations, the sky is totally cloudy during the whole simulation time (0000-2400 LT). In the two simulations assuming a homogeneous surface, the cloud-water mixing ratios are horizontal-uniformly distributed, for instance, in HOMG 0.124 g/kg and 0.557 g/kg at a height of 250 m and 450 m, respectively. In HOMS, the cloud-water amounts 0.108 g/kg and 0.556 g/kg at a height of 250 m and 450 m, respectively. Hence, all deviations from these distributions of cloud-water can be related to different land-use distributions. With increasing length of time, secondary differences may arise due to the differences in cloudiness, insolation and hence, modified evapotranspiration, as well as at differences in the advection of momentum, heat and moisture.

In section 5.1, the response of cloud-water to the underlying surface is exemplarly discussed at different levels for 1200 LT (Fig. 2). In section 5.2, focus is on the vertical cloud-water distribution (Figs. 3, 4.). In section 5.3, the temporal development of cloud-water is discussed (Figs. 5, 6).

No convincing response is found in simulations with strips parallel or perpendicular to the wind, independent of the strip size (xxxP25, xxxR25, xxxP5, xxxR5), as well as in simulations with a patch size of 5 km (xxxC5).

5.1. Horizontal Distribution of Cloud-Water

The cloud-water distribution obtained by the two homogeneous simulations (HOMG, HOMS) suggest that a homogeneous surface may lead to a homogeneous cloud-water distribution. Therefore, all structures in the distributions of cloud-water are due to the land-use distribution. In the following discussion, we focus on the height with the largest amount of cloud-water, which is 450 m. As pointed out above, in the simulation without vegetation at a height of 450 m, the amount of cloud-water (HOMS 0.557 g/kg) hardly differs from that in the simulation with vegetation (HOMG 0.556 g/kg).

Not all the simulations performed with heterogeneously covered surfaces show a clear response caused by the interactions between the neighbouring patches. Figure 2 shows an example of how cloud-water distribution may depend on land-use distribution.

Focusing on simulation SGSX25 in Fig. 2b, higher values of cloud-water were found above the homogeneous strip of *sand* oriented from west to east in the middle (between kilometre 25 and 50 in N-S-direction). Here, the larger sensible heat-fluxes, among others, enhance convection. The maximum of cloud-water occurring over the sandy patches can be explained as follows. The air lifts over the sandy patches and is replaced by moist air from the neighbouring *grass* patches that evapotranspirate at a higher rate than the sandy patches.

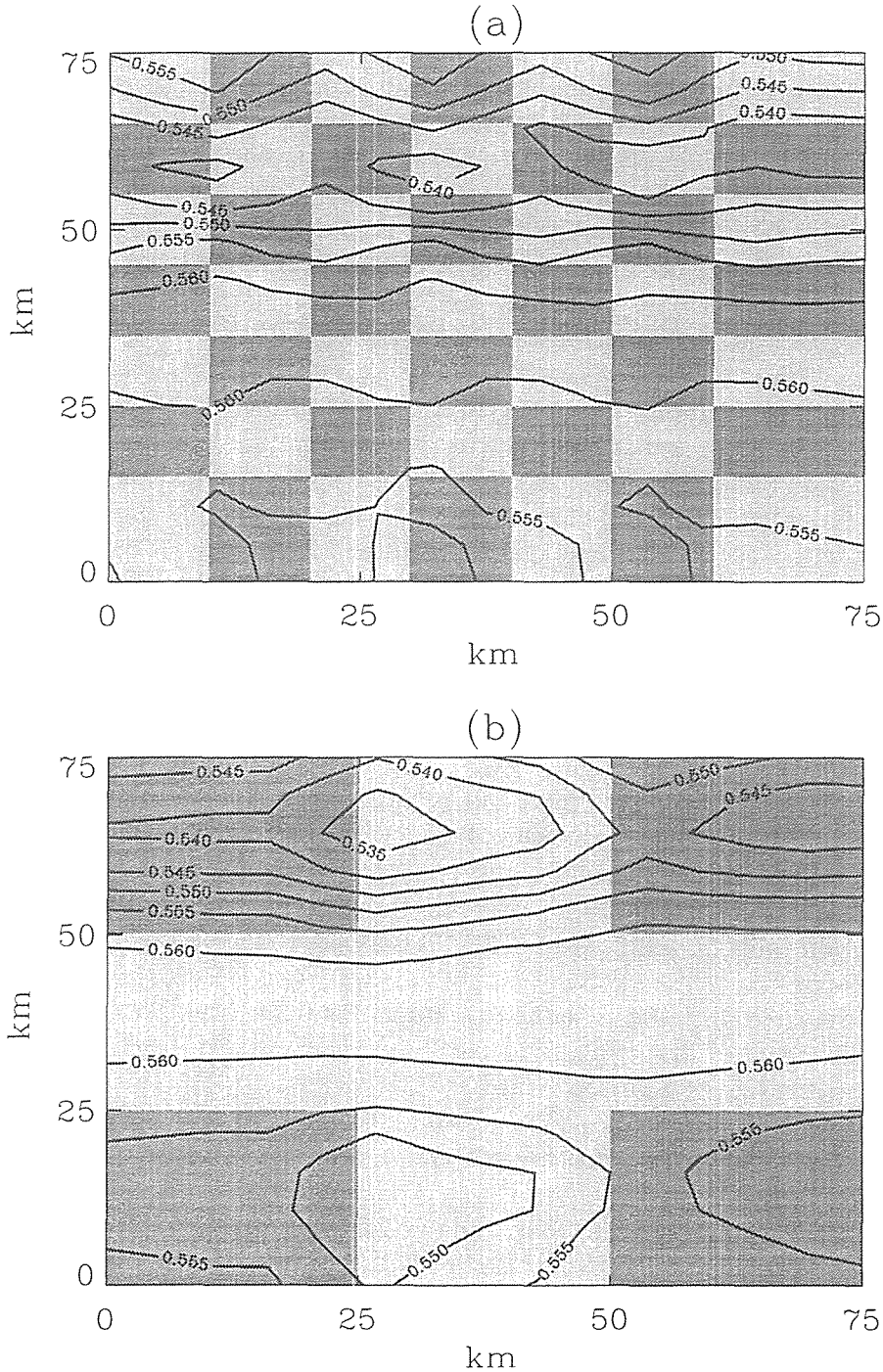

Fig. 2. Distribution of cloud-water mixing ratio at 1200 LT at a height of 450 m for the simulations (a) SGSC10 and (b) SGSX25, respectively. Grey patches indicate *grass* and light grey patches indicate *sand*, respectively.

Over the whole domain, there is a steady flow of 7m/s exist from west-southwest. On the other hand, there are lower values of cloud-water above the *sand* patches in the northern part (between km 50 to 75 in a NS-direction and km 25 to 50 in an EW-direction) and the southern part (between km 0 and 25 in a NS-direction and km 25 to 50 in an EW-direction) and there exist higher values above the *grass* patches at the northern and southern edges. This structure can be explained by advective effects. The different water supply is obvious slightly at a height of 450 m after the boundary between *grass* and *sand*. In the northern part as well as in the southern part, the amount of cloud-water decreases behind the patch covered by *grass* with 0.005-0.020 g/kg and increases after passing the *sand* 25 km long part with up to 0.010 g/kg.

Moisture convergence increases above the vegetationless parts. Therefore, the higher cloud-water values exist above the last passed *grass* covered corners.

Generally, in the case of heterogeneous surfaces, it seems that the vegetationless part creates a higher amount of cloud-water. However, on the contrary, the latent heat-flux of *grass* is larger than that of *sand*. Strong convection is found above *sand* patches. Only horizontal advection at the 450 m level and some interactions between the processes associated with the respective neighbouring patches yield in higher or lower values of cloud-water (e.g. Fig. 2b).

In GSGC10 (Fig. 2a), the amount of cloud-water is generally less than in the two simulations assuming homogeneous surfaces (HOMG and HOMS). In the northern strip going from west to east, the underlying surface clearly leads to an increase and a decrease of cloud-water after passing either a part with a *grass* or a *sand* surface. Further southwards, a direct decrease in the cloud-water mixing ratios is found above the *grass*-covered surface. The air with these lower amounts of cloud water is transported eastwards after passing a *grass* patch (similar as shown in Fig. 2b). In the middle east-west-orientated part of the domain (between 25 to 50 km in S-N-direction), there exist the highest values of cloud-water and a wave-like structure is formed (Fig. 2b). It seems that in this part and in the further northern and southern east-west orientated strip, the cloud-water distribution behaves as if the underlying land-use were homogeneous in this part. The amount and structure of cloud-water between 25 and 40 km in a NS direction is the same as in Fig. 2b. Therefore, a response is seen, but one cannot ascertain which type of land-use or which of the 10-km-by-10-km patches creates what amount of cloud-water.

5.2. Vertical Distribution of Cloud-Water

The amount of cloud-water increases from the lowest cloud-level at 250 m height to the highest cloud-level at a 450-m height by up to 0.4 g/kg. If, in the cloud-water distribution, structures are clearly visible at 250 m, they will disappear at higher levels and new structures will build up at 450 m. The largest changes in the cloud-water distribution with height are illustrated in Figs. 3 and 4.

In contrast to Fig. 2b, which represents the inverted patch arrangement of *grass* and *sand*, a flowing structure dominates in Fig. 3. In Fig. 3a, the maximum of cloud-water is found in the middle east-west-orientated strip. It is more than 0.020 g/kg higher than at the edges. It seems that this middle *grass* strip governs the distribution of cloud water at the northern and southern edges. Only in horizontal direction at 20 and 60 km in a north-south direction does an independent (from the middle *grass* strip) patch arrangement develop. The large and dominant amount of *grass* in the middle of GSGX25 provides less water vapour to the lower ABL than SGSX25 because of the slightly cooler air. Therefore, less cloud-water develops. The lower values of cloud-water over the *sand* patches at the corners can be explained by the overall lower relative humidity in this simulation and the slightly warmer air over the *sand* than over the *grass* which results in higher cloud bases above ground (Fig. 3b). Over the *grass* cross, more water evapotranspirates. A steady lifting (with no disturbance by a change in the underlying land-use) supports the formation of the maximum of cloud-water.

At 450 m, the cloud-water distribution has its maximum of 0.560 g/kg at the edges and its minimum of 0.515 g/kg at the interface between *sand* and *grass* at kilometre 50 in a NS direction (Fig. 3b.). A maximum of cloud-water occurs above the southern *sand-grass* boundary. A minimum of cloud-water exists at the interface of *grass-sand* at km 50 in an EW direction. Comparing Fig. 3b with Fig. 2b shows that not only the increased water-vapour supply but also the development of convective cells plays the important role. One sees that only small land-use changes -- for example, a change in the rotation of crops without a change in patch size -- leads to such a different development in clouds.

In the cloud-water distribution shown in Fig. 4b, considering the northern-, middle- and southern east-west-orientated strips, the higher values of cloud-water are found directly

over the northern and southern strips where more patches with vegetation exist than over the middle strip. When the wind passes over the alternating *grass* and *sand* patches, it seems that the cloud-water structures start to mix together.

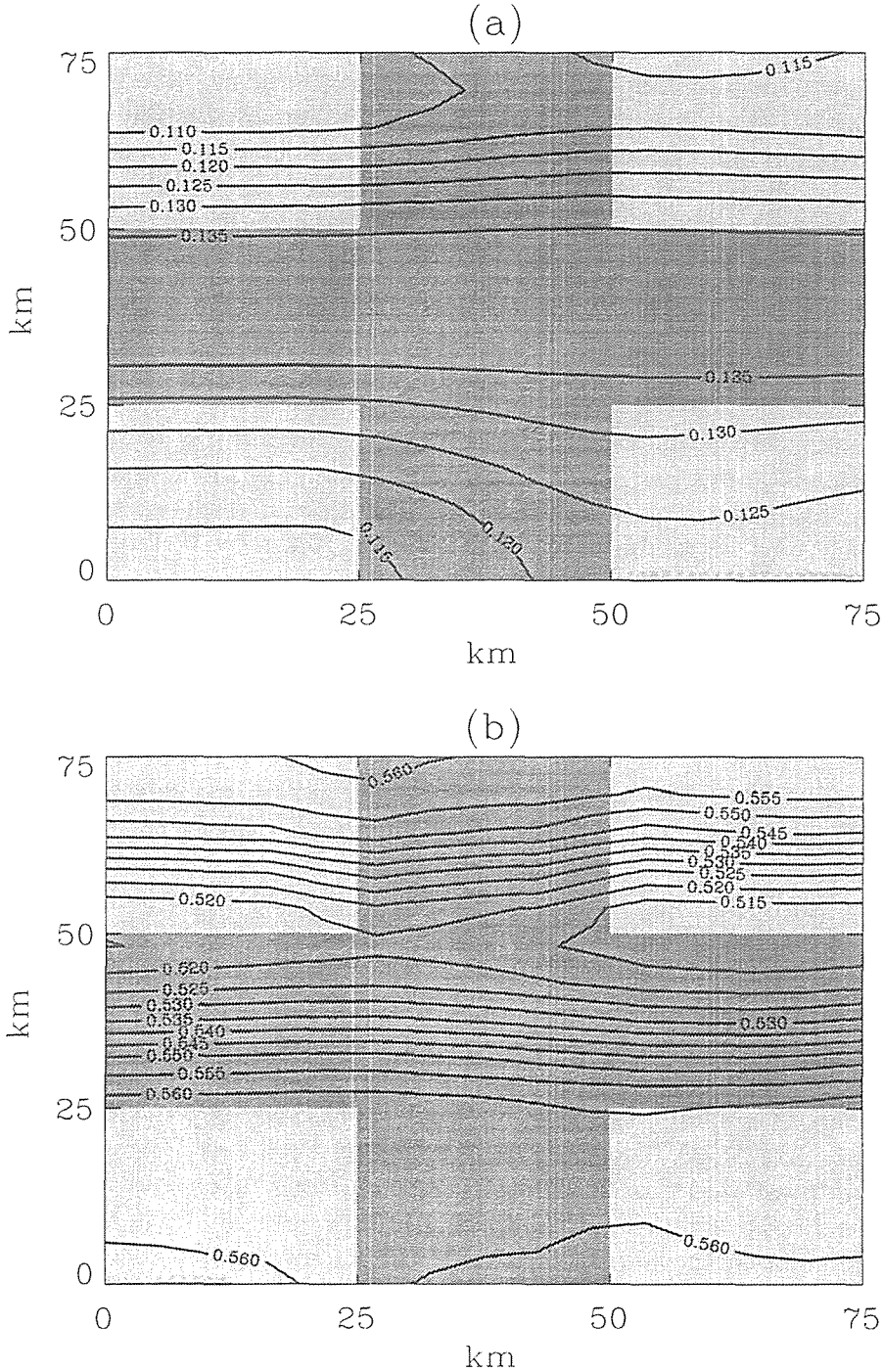

Fig. 3. Like Fig. 2, but distribution of cloud-water mixing ratio at 1200 LT for GSGX25 at (a) 250 m and (b) 450 m height, respectively.

At a height of 450 m, structures are similar to those in Fig. 2b. Surprisingly, over the heterogeneous strip in the middle (0 to 75 km in an east-west direction and 25 to 50 km in a north-south direction), the cloud-water distribution provides no response to the underlying surface, while at the edges it does. If the moisture convergence is strong, clouds can build over the *sand*-dominated parts in the middle. On the other hand, above the northern and southern *sand*

patches (similar to Fig. 2b), the minimum of cloud-water goes along with the maximum of sensible heat-flux. This is due to the dominance of the surrounded *grass* patches and advective effects.

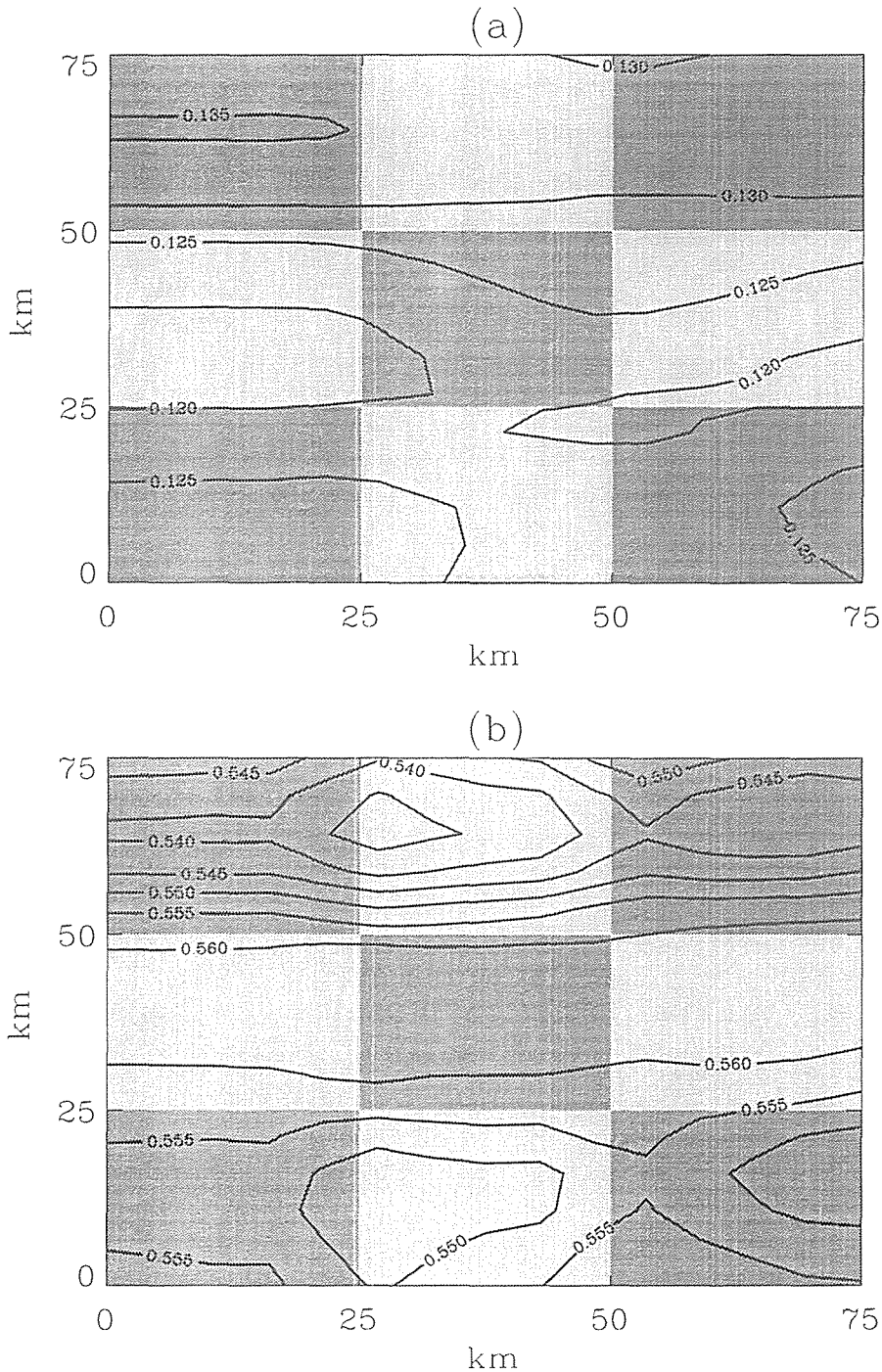

Fig. 4. Like Fig. 2, but distribution of cloud-water mixing ratio at 1200 LT for GSGC25 at (a) 250 m and (b) 450 m height, respectively.

5.3. Temporal Development of Cloud-Water Distribution

In this subsection, we consider the temporal cloud-development (Fig. 5, Fig. 6) and the amount of daily sums of the domain-averaged of cloud-water between the level of 250 m and

450 m (Tab. 3), which can be related to the evapotranspiration over the 24 hours of simulation (Tab. 2).

When comparing the amount of cloud-water at a height of 450 m in simulation SGSC10 at 1200 LT (Fig. 2a), 1500 LT (Fig. 5a) and 1800 LT (Fig. 5b), a clear response of the cloud-water mixing ratios to the heterogeneity of the underlying surface can be found at 1200 LT.

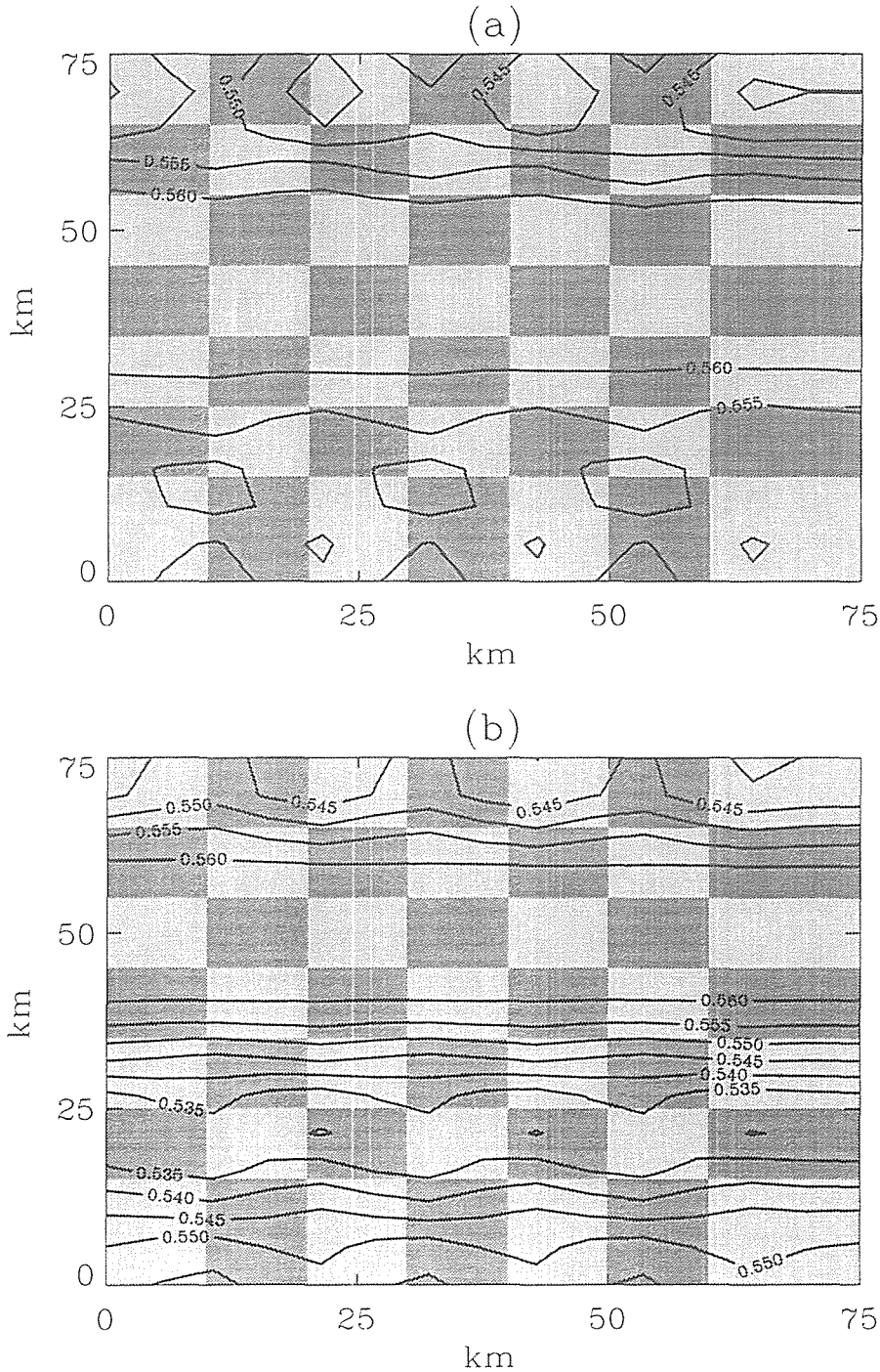

Fig. 5. Like Fig. 2, but distribution of cloud-water mixing ratio for SGSC10 at a height of 450 m at (a) 1500 LT and (b) 1800 LT, respectively. Note that the cloud-water distribution at 1200 LT for the same simulation in the same height is shown in Fig. 2.

The amount of cloud water goes along with the net radiation and, therefore, with the magnitude of the sensible and latent heat-fluxes. The increased latent heat-fluxes enhance cloud formation (positive feedback). Later on, this enhanced cloudiness reduces insolation and

hence the fluxes of sensible and latent heat (negative feedback), which again lead to less cloud water formation.

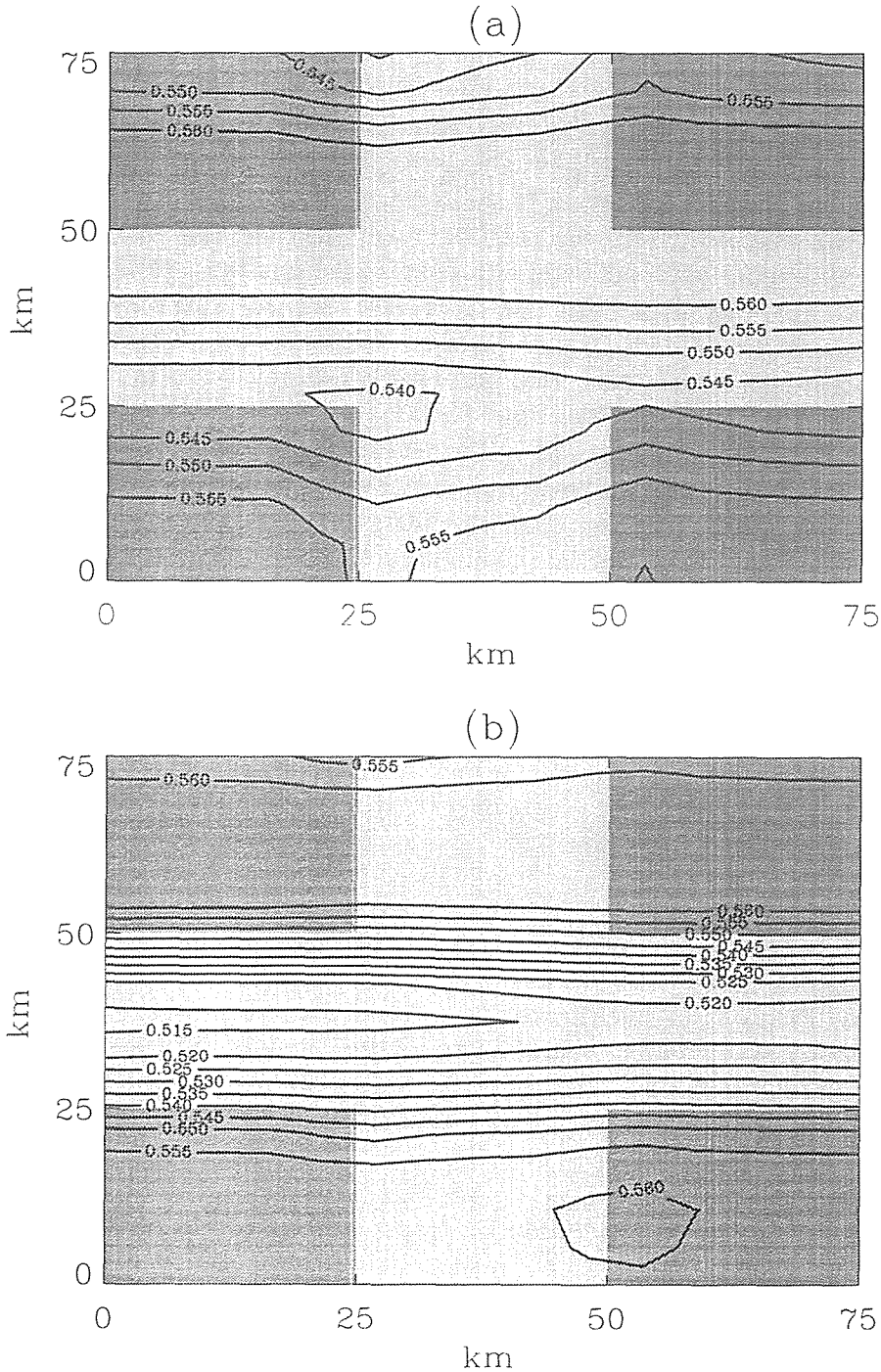

Fig. 6. Like Fig. 2, but distribution of cloud-water mixing ratio for simulation SGSX10 at a height of 450 m at (a) 1500 LT and (b) 1800 LT, respectively. Note that the cloud-water distribution at 1200 LT for the same simulation in the same height is shown in Fig. 2.

During all simulations the sun rises at 0600 LT. The maximal net radiation appears at 1200 LT. Furthermore, the maximum of the domain-averaged latent heat-fluxes of SGSC10 appears at 1300 LT with about 42 W/m² (Friedrich and Mölders, 1998). The maximum of the domain averaged sensible heat-flux appears also at 1300 LT. This maximum fits perfectly with the increase of cloud-water maximum of 0.56 g/kg from 1200 LT to 1500 LT.

Between 1200 LT and 1500 LT the maximum of cloud-water (0.560 g/kg) reaches from a 20-km strip in the middle at 1200 LT (Fig. 2a) to a 30-km strip at 1500 LT (Fig. 5a). The square patches with lower values of cloud-water are forced north- and southwards, respectively. Between 1500 LT and 1800 LT the amount of cloud-water decreases with the decrease of the domain-averaged latent heat-flux ($\Delta LE = 29$ W/m²).

A similar behaviour in the distribution of cloud-water patches with processing time occurs in SGSX25. At 1200 LT (Fig. 2b), patches with large amounts of cloud-water are found in the northern and southern parts above the *sand* patches (Fig. 2b). These large cloud-water mixing ratios can be lead back to the formation of strong upward motions above the *sand* and a horizontal flow from the neighbouring *grass* patches (see subsection 5.1). The maximum in the amount of cloud-water occurring in the middle *sand* strip resembles a maximum in sensible heat-flux at 1200 LT above the *sand* strip and a maximum in latent heat-flux above the *grass*-corners (Friedrich and Mölders, 1998). In the northern and southern *sand* patches, the latent heat-fluxes increase slightly behind kilometre 40 in an east-west direction. The amount of cloud-water increases until 1500 LT (Fig. 6a). This increase goes along with the maximum in the domain-averaged latent heat-flux at 1300 LT. It might continue at the expense of clearly developed cloud-water patches caused by the heterogeneity of the underlying land-use, which have nearly vanished at 1500 LT (Fig. 6a). At 1200 LT, the maximum of cloud-water occurring above the *sand* strip in an EW-direction at the interface between vegetation and *sand* at kilometre 40 to 60 in a NS direction is displaced northwards with processing time, followed by the minimum of cloud-water (0.545-0.540g/kg) between kilometre 20 to 30 in a NS direction. The strong vertical motion occurring over the *sand* breaks down in the late afternoon. Therefore, a displacement of the maximum of cloud-water is expected towards the *grass*-covered parts. Accordingly, the highest values of cloud-water occur at 1800 LT in the *grass*-covered parts, while over the sandy parts the cloud-water amount decreases rapidly. Surprisingly, in the northern and southern parts the *sand* patches have no influence on the amount cloud-water at 450 m height.

5.3.1. The Daily Sums of Domain-Averaged Cloud-Water

When comparing the daily sums of the domain-averaged latent heat-fluxes (Tab. 2) with those of cloud-water (Tab. 3), a correlation is found between the water vapour supply to the atmosphere by turbulent latent heat-fluxes and the amount of cloud-water in simulation SGSX25 and SGSC25. For instance, SGSX25 (Figs. 2a, 6a, b) evapotranspirates the second highest amount of water and is the simulation with the largest amount of cloud-water during the whole day and at all levels.

Although simulations SGSX25 (44.4 % *grass*), SGSC25 (44.4 % *grass*) as well as SGSC5 (49.8 % *grass*) have less vegetation compared to the simulation with a homogeneous *grass* cover HOMG (100 % *grass*), the amount of daily sums of the domain-averaged cloud-water is much higher due to the enhanced convection. On the other hand, the counterparts of these simulations, namely, GSGC25 (55.6 % *grass*), and GSGX25 (55.6 % *grass*) provide the same amount of cloud-water as HOMS. The differential in the daily sums of the domain-averaged cloud-water between GSGC25 and GSGX25 to SGSC25 and SGSX25 exceeds 0.8 g/(kg*d). These differences suggest that not the amount of land-use, but the land-use distribution plays the major role in the development of cloud structures.

The results of GSGC10 and SGSC10 are similar to those of the simulations which assume nearly the same amounts of *grass* (52 % *grass* and 48 % *grass*, respectively). Here the differential in the daily sums of the domain-averaged cloud-water is about 0.31 g/(kg*d). The greater importance of the land-use distribution than that of the fractional coverage by vegetation is also manifested by the differences in the daily sums of the domain-averaged cloud-water between HOMG and HOMS, which is only 0.14 g/(kg*d), although *grass* evapotranspirates more water than *sand*.

Tab. 2. Differentials of all simulations. The grey squares are the daily sums of the domain-averaged latent heat-flux, while the values below this indicate the left column minus the top row and the values above the daily- and domain-sums of values are the top row subtracted from the left column, respectively. Because of space limitations, all names have been shortened to the first two letters. Therefore, the first letter stands for the dominant land-use followed by the sign of the orientation of the patch and finally the length of the patch, respectively.

*W/(m²*d)*	*HOMG*	*SX25*	*SC25*	*GP25*	*SP25*	*GR25*	*SR5*	*GP5*	*GC25*	*SP5*	*GC5*	*SC10*	*GC10*	*GX25*	*SC5*	*SR25*	*GR5*	*HOMS*
HOMG	**404.6**	-7.7	-18.5	-25.3	-26.1	-31	-35	-36	-36	-36	-39	-39	-42.8	-45.7	-52	-59.3	-61	-88
SX25	-7.7	**396.9**	-10.8	-17.6	-18.4	-23.3	-27	-28	-28.3	-29	-31	-31	-35.1	-38	-44	-51.6	-53	-80
SC25	-18.5	-10.8	**386**	-6.8	-7.6	-12.5	-16	-17	-17.5	-18	-20	-20	-24.3	-27.2	-33	-40.8	-42	-70
GP25	-25.3	-17.6	-6.8	**379**	-0.8	-5.7	-9.2	-10	-10.7	-11	-13	-13	-17.5	-20.4	-26	-34	-35	-63
SP25	-26.1	-18.4	-7.6	-0.8	**379**	-4.9	-8.4	-9.6	-9.9	-10	-12	-13	-16.7	-19.6	-26	-33.2	-35	-62
GR25	-31	-23.3	-12.5	-5.7	-4.9	**374**	-3.5	-4.7	-5	-5.2	-7.5	-7.6	-11.8	-14.7	-21	-28.3	-30	-57
SR5	-34.5	-26.8	-16	-9.2	-8.4	-3.5	**370**	-1.2	-1.5	-1.7	-4	-4.1	-8.3	-11.2	-17	-24.8	-26	-54
GP5	-35.7	-28	-17.2	-10.4	-9.6	-4.7	-1.2	**369**	-0.3	-0.5	-2.8	-2.9	-7.1	-10	-16	-23.6	-25	-52
GC25	-36	-28.3	-17.5	-10.7	-9.9	-5	-1.5	-0.3	**369**	-0.2	-2.5	-2.6	-6.8	-9.7	-16	-23.3	-25	-52
SP5	-36.2	-28.5	-17.7	-10.9	-10.1	-5.2	-1.7	-0.5	-0.2	**368**	-2.3	-2.4	-6.6	-9.5	-15	-23.1	-25	-52
GC5	-38.5	-30.8	-20	-13.2	-12.4	-7.5	-4	-2.8	-2.5	-2.3	**366**	-0.1	-4.3	-7.2	-13	-20.8	-22	-50
SC10	-38.6	-30.9	-20.1	-13.3	-12.5	-7.6	-4.1	-2.9	-2.6	-2.4	-0.1	**366**	-4.2	-7.1	-13	-20.7	-22	-49
GC10	-42.8	-35.1	-24.3	-17.5	-16.7	-11.8	-8.3	-7.1	-6.8	-6.6	-4.3	-4.2	**362**	-2.9	-8.8	-16.5	-18	-45
GX25	-45.7	-38	-27.2	-20.4	-19.6	-14.7	-11	-10	-9.7	-9.5	-7.2	-7.1	-2.9	**359**	-5.9	-13.6	-15	-42
SC5	-51.6	-43.9	-33.1	-26.3	-25.5	-20.6	-17	-16	-15.6	-15	-13	-13	-8.8	-5.9	**353**	-7.7	-9.1	-36
SR25	-59.3	-51.6	-40.8	-34	-33.2	-28.3	-25	-24	-23.3	-23	-21	-21	-16.5	-13.6	-7.7	**345**	-1.4	-29
GR5	-60.7	-53	-42.2	-35.4	-34.6	-29.7	-26	-25	-24.7	-25	-22	-22	-17.9	-15	-9.1	-1.4	**344**	-27
HOMS	-88	-80.3	-69.5	-62.7	-61.9	-57	-54	-52	-52	-52	-50	-49	-45.2	-42.3	-36	-28.7	-27	**317**

6. Summary and Conclusion

Under the meteorological situation assumed in this case study, an obvious relationship exists between the development or the underlying surface and the distribution of cloud-water for a homogeneous patch size of 25 by 25 km². Herein, the land-use pattern may be squares, crosses or diamonds, but not strips which are parallel or perpendicular to the wind. Patch sizes between 25 by 25 km² and 10 by 10 km² provide a response which cannot clearly be related to the underlying surface, while simulations with a patch size smaller than 10 by 10 km² do not show any response to the land-use distribution. The amount of cloud-water does not depend primarily on the amount of a certain land-use. Large *sand* patches are able to force the required upward motions due to large fluxes of sensible heat. Nevertheless, adjacent wet patches are necessary to provide sufficient moisture by latent heat-fluxes for cloud formation over the *sand* patches (moisture convergence). Furthermore, all together, the amount of land-use, the distribution and the interaction between the neighbouring patches are responsible for the cloud-water distribution at a certain level.

Additionally, the amount of cloud-water also agrees with the maximum of latent- and sensible heat-flux and with the radiation heat-flux. Therefore, the amount of cloud-water, independent of the patch size and arrangement, increases until 1200 or 1300 LT, which goes along with the maximum of latent and sensible heat-fluxes, and decreases toward the evening hours. The structure of the cloud-water distribution changes depending on the patch arrangement and patch size in the course of time.

A relation between the maximum of the daily sums of the domain-averaged latent heat-fluxes and the maximum of the amount of cloud-water (Tabs. 2, 3) is only found in SGSX25 and SGSC25. In all other simulations, the amount of cloud-water and the cloud structures seem to have no obvious dependency on the land-use distribution. Furthermore, simulations with well-balanced equal parts of wet/cool and dry/warm parts that supply water-vapour and heat have higher daily sums of domain-averaged cloud-water. The results of GSGC25 (55.6 % *grass*) and GSGX25 (55.6 % *grass*), which have the same percentage of *grass* and *sand* but different land-use distribution, prove that in some cases the land-use distribution may be of much more importance than the amount of land-use for the daily amount of cloud-water. This fact is also substantiated by the results of simulations where the percentage of land-use differs only slightly (e.g. GSGC10 and SGSC10 with 52 % *grass* and 48 % *grass*, respectively). Despite nearly the same percentage of land-use, the daily sums of domain-averaged cloud-water differ about 0.31 g/(kg*d).

7. Acknowledgements

This study was supported financially by the DFG under contracts Mo770/1-1 and Mo770/1-2 and by the BMBF under contract LT2.D.2. Furthermore, we thank Dr. Christoph Jacobi for his helpful remarks and suggestions.

8. References

Anthes, R.A., 1984. Enhancement of convective precipitation by mesoscale variations in vegetative covering in semiarid regions. *J. Clim. and Appl. Met.* **23**, 541-554.

Avissar, R., R.A. Pielke, 1989. A parameterization of heterogeneous land surface for atmospheric numerical models and its impact on regional meteorology. *Mon. Wea. Rev.* **117**, 2113-2136.

Deardorff, J.W., 1978. Efficient prediction of ground surface temperature and moisture, with

inclusion of a layer of vegetation. *J. Geophys. Res.* **84C**, 1889-1903.

Eppel, D.P., H. Kapitza, M. Claussen, D. Jacob, W. Koch, L. Levkov, H.-T. Mengelkamp, N. Werrmann, 1995. The non-hydrostatic mesoscale model GESIMA. Part II: Parameterizations and applications. *Contrib. Atmos. Phys.* **68**, 15-41.

Friedrich, K., Mölders, N., 1998. A numerical case study on the sensitivity of the water and energy fluxes to the heterogeneity of the distribution of landuse. In: Raabe, A., Arnold, K., Heintzenberg, J., Meteorologische Arbeiten aus Leipzig (III), Wiss. Mitt., 55-74.

Jürrens, R. 1996. Parametrisierung der Gebietsverdunstung zur Verwendung in meso- und makroskaligen meteorologischen Simulationemodellen. *Berichte des Instituts für Meterorologie und Klimatologie der Universität Hannover*, **53**

Kapitza, H., D.P. Eppel, 1992. The non-hydrostatic mesoscale model GESIMA. Part I: Dynamical equations and tests. *Contr. Phys. Atmos.* 65, 129-146.

Kramm, G., R. Dlugi, D.J. Dollard, T. Foken, N. Mölders, H. Müller, W. Seiler, H. Sievering, 1995. On the dry deposition of ozone and reactive nitrogen compounds. *Atmos. Environ.* 29, 3209-3231.

Mahrt, L., J. Sun, D. Vickers, J.I. MacPherson, J.R. Pederson, 1994. Ozone fluxes over patchy cultivated surface. *J. Geophys. Res.* **100D**, 23125-23131.

Mölders, N., A. Raabe, 1996. Numerical investigations on the influence of subgrid-scale surface heterogeneity on evapotranspiration and cloud processes. *J. Appl. Meteor.* **35**, 782-795.

Mölders, N., G. Kramm, M. Laube, A. Raabe, 1997. On the influence of bulk parameterization schemes of cloud relevant microphysics on the predicted water cycle relevant quantities - a case study. *Meteorol. Zeischr.* **6**, 21-32.

Mölders, N., 1998. On the influence of the geostrophic wind direction on the atmospheric response to landuse changes. In: Raabe, A., Arnold, K., Heintzenberg, J., Meteorologische Arbeiten aus Leipzig (III), Wiss. Mitt., 35-54.

Shuttleworth, W.J., 1991. Insight from large-scale observational studies on land/atmosphere interactions. *Surveys in Geophysics* 12, 3-30.

Address of the authors:

LIM - Institut für Meteorologie
Universität Leipzig
Stephanstraße 3
04103 Leipzig
Germany